Shape-Tunable Hollow Silica Nanomaterials Based on a Soft-Templating Method and Their Application as a Drug Carrier

Jiao Chen,[†] Xu Wu,[†] Xiaodong Hou,[†] Xingguang Su,[‡] Qianli Chu,[†] Nenny Fahruddin,[†] and Julia Xiaojun Zhao*,[†]

[†]Department of Chemistry, University of North Dakota, Grand Forks, North Dakota 58202, United States
[‡]Department of Analytical Chemistry, College of Chemistry, Jilin University, Changchun 130012, P. R. China

ABSTRACT: A one-step soft-templating method for synthesizing shape-tunable hollow silica nanomaterials was developed in a reliable and highly reproducible way. For the first time, both nonspherical and spherical shapes with hollow interiors, including nanowire, nanospheres, and nanotadpole, were successfully obtained by simply changing the solvent. Poly(vinylpyrrolidone) (PVP)−water droplets were used as soft templates for the formation of hollow structures, while three different solvents, including 1-propanol, 1-pentanol, and ethanol, led to the designed shapes. It was found that the solvent, the formation of PVP−water droplets, the amount of ammonia, and the reaction time had great effects on the morphology of synthesized hollow nanomaterials. The effect of various factors on the morphology was systematically studied to propose a growth mechanism. The obtained hollow silica nanomaterials showed excellent reproducibility and great potential for a large-scale synthesis. Finally, the application of the developed hollow silica nanomaterials was demonstrated using the hollow spherical silica nanoparticles. Its drug-carrying ability was studied. The results could be extended for doping various target molecules into the hollow structures for a broad range of applications.

KEYWORDS: hollow silica nanomaterials, soft-templating, shape-tunable, PVP, solvent, drug carrier
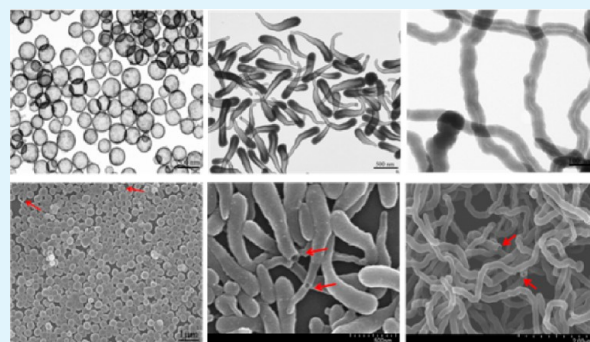
1. INTRODUCTION

Hollow silica nanomaterials (HSNs) have attracted noticeable attention because of their excellent biocompatibility, easy surface functionalization accessibility, good chemical inertness, and thermal stability.[1−8] They have been used in diverse fields including drug delivery, sensing, catalysis, and large biomolecular release.[9−11] The approaches for synthesizing HSNs can be broadly divided into two categories: hard templating[12−16] and soft templating.[17−19] The hard-templating method normally needs a layer of the desired materials coated on the surface of the template core, followed by the selective removal of the template. This approach has been widely used and proven to be effective for the synthesis of hollow nanomaterials with controllable shell thickness. However, tedious and complicated procedures are usually required, which are sometimes expensive and unsuitable for large-scale synthesis. Many efforts have been devoted to developing self-templating methods. In the soft-templating method, no additional templates are needed, and therefore it may have the advantage of a simple synthetic process and better scalability. For example, Wang and Zeng applied a novel microemulsion system to synthesize hollow silica nanoparticles, in which 1-dodecanethiol served as an oil phase in the "oil-in-water" emulsion and a soft template for the hollow interior. Moreover, the central space of the SiO₂ spheres was tunable by varying the amount of DDT.[20]

On the other hand, the HSNs obtained by soft-templating methods are mostly spherical in morphology. The preparation of well-defined hollow nonspherical nanomaterials with tunable sizes and morphologies by hard-templating methods generally introduces additional challenges because of the difficulties in forming a uniform coating around high-curvature surfaces and the deficiency of appropriate nonspherical templates. Therefore, the ability to tune the structure, size, and morphology of the synthesized nanomaterials is an important goal in current material synthesis and device fabrication.[21,22] Recently, Chen et al. developed a method to synthesize silica nanotubes based on the thermolysis of silicon tetraacetate with the assistance of both hard and soft templates.[23] Wu et al. found that rodlike hollow silica particles could be obtained by using a surfactant mixture composed of zwitterionic and anionic surfactants as the templates with the assistance of a constructure-directing agent.[24] These nonspherical new members expand the versatility of the hollow nanomaterials family and bring some novel properties, functions, and potential applications. However, the preparation of nonspherical nanomaterials generally requires strict reaction conditions in addition to high cost and

tedious synthetic procedures. Moreover, the morphology of the synthesized nanomaterial is not tunable.

Herein, we developed a synthetic approach for making HSNs with tunable morphologies by using poly(vinylpyrrolidone)−water droplets as the soft templates. Three morphologies with hollow interiors, including tadpole-like, wirelike, and sphere, were obtained easily by changing the applied solvent from 1-propanol, to 1-pentanol, to ethanol, respectively. In addition, we demonstrated that the molar ratio of NH_4OH to TEOS and the reaction time could also be used as factors to tune the morphology of produced nanomaterials. The effect of various factors on the morphology was systematically studied to propose a growth mechanism. The potential application of the developed hollow nanomaterials was investigated by taking the hollow spherical silica nanomaterials (HSSNs) as an example to study its drug-carrying ability. Using inexpensive and commercially available reagents, the newly developed one-step synthetic strategy shows significantly high reproducibility that brings great potential for a large-scale synthesis.

2. EXPERIMENTAL SECTION

2.1. Materials. Tetraethylorthosilicate (TEOS; 98%) was purchased from Aldrich. Ammonium hydroxide (28.0−30.0%), absolute ethanol (EtOH; 99%), and EtOH (95%) were obtained from Fisher Scientific Co. Sodium citrate (Na_3Ct), 1-propanol, 1-pentanol, and poly(vinylpyrrolidone) (PVP; average molecular weight M_n = 40000) were purchased from Alfa Aesar. Tris(bipyridine)-ruthenium(II) dichloride (Rubpy) was purchased from ICN Biomedicals Inc. *Escherichia coli* HB101 strain [genotype: F-, *thi*-1, *hsd*S20 (rB⁻, mB⁻), *sup*E44, *rec*A13, *ara*-14, *leu*B6, *pro*A2, *lac*Y1, *gal*K2, *rps*L20(str^r), *xyl*-5, *mtl*-1] was obtained from American Tissue Culture Collection, and polymyxin B was purchased from MPBio. Deionized water (H_2O; Millipore, Milli-Q grade) with a resistivity of 18.2 MΩ·cm was used in all experiments.

2.2. Characterization. A Hitachi 7500 transmission electron microscope (TEM) and a Hitachi SU8010 field-emission scanning electron microscope (SEM) were used to take images of the developed silica nanomaterials. The fluorescence intensities of the synthesized fluorescent silica nanomaterials were measured using a Jobin Yvon Horiba Fluorolog spectrofluorimeter. The Carl Zeiss LSM 510 Meta laser scanning confocal microscope was used to observe Rubpy-doped hollow silica nanoparticles. Elemental analysis was achieved by performing energy-dispersive X-ray spectroscopy measurements using an Oxford X-Max energy-dispersive X-ray spectrometer (EDS) that is attached to the Hitachi SU8010 field-emission SEM. Powder X-ray diffraction (XRD) patterns of the synthesized nanomaterials were recorded on a Rigaku Ultima IV diffractometer with *PDXL* software. The diffraction patterns were collected at room temperature using Ni-filtered Cu Kα radiation of wavelength 1.5408 Å with an accelerating voltage of 40 kV and an emission current of 44 mA. The angle regions were scanned from 10 to 80° (2θ) with a step size of 0.02° at a scan rate of 1°/min. The Beckman DU 640 spectrophotometer was used to measure the optical density (OD) of the LB bacterial suspensions in the kinetic study for determination of the bacterial growth curve.

2.3. Synthesis of Hollow Nonspherical Silica Nanomaterials (HNSNs). *2.3.1. Synthesis of Hollow Silica Tadpole-like Nanomaterials.* Monodispersed hollow silica tadpole-like nanomaterials were prepared by using 1-propanol as the solvent. A mixture of 3.00 g of PVP and 30.00 mL of 1-propanol was sonicated for 30 min until all PVP was dissolved. An aliquot of 3.00 mL of 95% EtOH, 0.84 mL of H_2O, and 0.20 mL of 0.17 M Na_3Ct was added into the PVP/1-propanol mixture and gently shaken by hand, followed by the addition of 0.30 mL of TEOS and 0.60 mL of NH_4OH. The mixture was left to rest, and the reaction was allowed to proceed overnight at room temperature. The tadpole-like nanomaterials were collected by centrifuging at 3000 rpm for 30 min. The supernatant was removed, and the precipitates were washed three times with EtOH for 20 min at a centrifuging speed of 3000 rpm.

2.3.2. Synthesis of Hollow Silica Nanowires (HSiNWs). The synthetic procedures were the same as those used in the synthesis of hollow tadpole-like nanomaterials except that the solvent was changed from 1-propanol to 1-pentanol and 0.10 mL instead of 0.60 mL of NH_4OH was added. When the molar ratio of NH_4OH to TEOS is changed from 0.53, 1.60, 2.67, 3.73, 4.80, to 5.87, different shapes of silica nanomaterials can be obtained.

2.4. Synthesis of HSSNs. Monodispersed HSSNs were prepared using EtOH as the solvent. A total of 0.50 g of PVP was added to 10.00 mL of absolute EtOH, and the mixture was sonicated until all of the PVP was dissolved. A 0.40 mL aliquot of H_2O and 0.10 mL of 0.17 M Na_3Ct were added into the PVP−EtOH mixture, followed by the addition of 0.40 mL of NH_4OH and 0.15 mL of TEOS. The mixture was shaken by hand gently and then left to rest for overnight reaction at room temperature. HSSNs were collected by centrifuging at 3000 rpm for 30 min. The supernatant was removed, and the precipitates were washed three times with EtOH for 20 min. The calcination process at 500−600 °C for 4 h can remove PVP to obtain HSSNs.[25] For the synthesis of dye-doped HSSNs, 0.40 mL of a 10.00 mM Rubpy solution was added instead of 0.40 mL of H_2O, and the reaction proceeded in the dark. Rubpy-doped HSSNs were collected by centrifuging at 3000 rpm for 30 min, and the precipitates were washed three times by EtOH. After carefully removal of the supernatant, the Rubpy-doped HSSNs were redispersed in 10 mL of H_2O for fluorescence intensity measurement. The fluorescence intensities of a pure Rubpy aqueous solution (0.03 mM) and pure HSSNs (0.05 mg/mL) were measured as controls. For the synthesis of polymyxin B-doped HSSNs, 0.40 mL of a 5.00 mg/mL polymyxin B solution was added instead of 0.40 mL of H_2O.

2.5. Monitoring of the Formation Process of the HSNs at Different Reaction Times. The intermediates of the hollow nanomaterials were collected at different reaction times to study their formation process. The synthetic procedures were the same as those described in section 2.4. When using 1-propanol as the solvent, a 5.00 mL aliquot of a synthetic solution was collected when the reaction had proceeded for 5 min, 10 min, 1 h, and 16 h; the same amount was also taken at 1, 2, 3, 5, and 16 h with 1-pentanol as the solvent. A 5.00 mL aliquot of acetone or EtOH was added to the collected solutions and then centrifuged at 3000 rpm for 30 min, and the supernatant was subsequently removed. The precipitates were washed three times by EtOH and redispersed in distilled H_2O.

2.6. Antibacterial Experiments in LB Plates. A 0.05 mL aliquot of an *E. coli* suspension was mixed with 0.05 mL of 2.00 mg/mL HSSNs, pure H_2O, or polymyxin B-doped HSSNs with a concentration of 1.00, 0.50, 0.25, and 0.10 mg/mL, respectively. Each as-prepared 0.10 mL bacteria−sample mixture was evenly spread on the surface of LB-agar dishes. The dishes were then placed in an incubator for 24 h at 37 °C.

2.7. Bacterial Kinetic Study. A 0.05 mL aliquot of an *E. coli* suspension was added to 5.00 mL of LB, followed by the addition of different samples. The final concentrations of the samples were 0.040 mg/mL pure HSSNs and 0.005, 0.020, and 0.100 mg/mL polymyxin B-doped HSSNs. H_2O and pure HSSNs were used as controls. The initial time of adding each sample to a LB bacterial suspension was recorded as zero. The suspension was incubated at 37 °C at a shaking speed of 200 rpm. At each set time interval, a 0.20 mL aliquot of the suspension was withdrawn from the incubator and placed in a cuvette containing 1.80 mL of LB broth. Then, an OD measurement at a wavelength of 600 nm was performed to estimate the amount of bacteria present in the samples.

3. RESULTS AND DISCUSSION

3.1. Synthesis of HNSNs. Two distinct morphological nonspherical silica nanomaterials, hollow tadpole-like and HSiNWs, were obtained by using 1-propanol and 1-pentanol as the solvent, respectively. In a typical synthetic process, PVP was first dissolved in the solvent, followed by the addition of EtOH, Na_3Ct, H_2O, NH_4OH, and TEOS, in which EtOH was used as the cosolvent, Na_3Ct as the stabilizer, and NH_4OH as
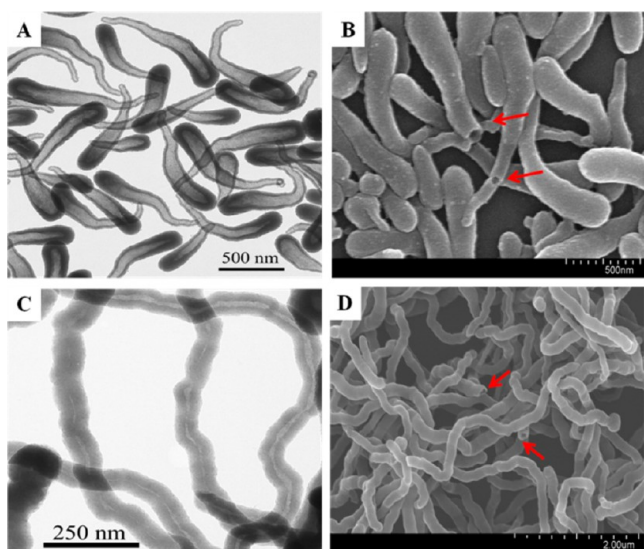
Figure 1. TEM and SEM images of obtained hollow silica tadpole-like nanomaterials (A and B) and HSiNWs (C and D) by using 1-propanol or 1-pentanol as the solvent, respectively. TEM images: A and C. SEM images: B and D.

the catalyst. The formation of a silica shell was initiated by the addition of TEOS, which acted as the silica precursor.

When 1-propanol was used as the solvent, the resulting hollow nanomaterials showed a tadpole-like shape (Figure 1A,B). They possessed a relatively round shape at one end, resembling the head of a tadpole, and the hollow structure gradually became thinner toward the other end, resembling the tail of a tadpole. The average diameter of the head parts was 235 ± 35 nm with a silica shell thickness of 58 ± 9 nm. The diameter and silica shell thickness of the tail parts were 64 ± 5 and 23 ± 5 nm, respectively. The shape of the product was uniform. Over 99% of the produced nanomaterials had the tadpole-like morphology. The hollow structure can be clearly observed from both the TEM image (Figure 1A) and the broken nanomaterials in the SEM image (Figure 1B, red arrows).

Ultralong HSiNWs were obtained when the solvent was changed to 1-pentanol, as shown in Figure 1C,D. The nanowires have a typical length of up to tens of micrometers and a diameter ranging from 60 to 100 nm. The hollow structures can be clearly observed either from the TEM (Figure 1C) or some broken HSiNWs in the SEM image (Figure 1D,

red arrows). It is also worth noting that the HSiNWs can bend dramatically without breaking into small pieces, showing their excellent flexibility.

The chemical composition and crystalline property of the HSNs were investigated using EDS elemental analysis and powder XRD patterns. The hollow nanomaterials with different shapes showed similar chemical composition and crystalline property. Here the results for the HSiNWs were presented as an example. The EDS spectrum in Figure 2A was obtained from a single nanowire of the indicated yellow area on the SEM image (Figure 2A, inset). EDS analysis demonstrated that the nanowire contained Si and O with an approximate atomic ratio of Si:O = 1:2. Apart from Si and O signals, peaks of Al and Na were also detected, which was from the SEM sample supporter (made of Al) and residue of the synthesis (the addition of Na_3Ct in the synthesis of silica nanowire). The XRD pattern of the synthesized HSiNWs is shown in Figure 2B. The scattering pattern exhibited one broad peak ranging from 15 to 30° with the peak value at a 2θ angle of 24°, indicating the amorphous nature of the HSiNWs. It was reported that one-dimensional amorphous HSiNWs are good candidates for photoluminescent materials because of their unique blue-light emission.[26−30] Therefore, the amorphous characteristic of the prepared HSiNWs may have potential applications in nanoelectronic devices.
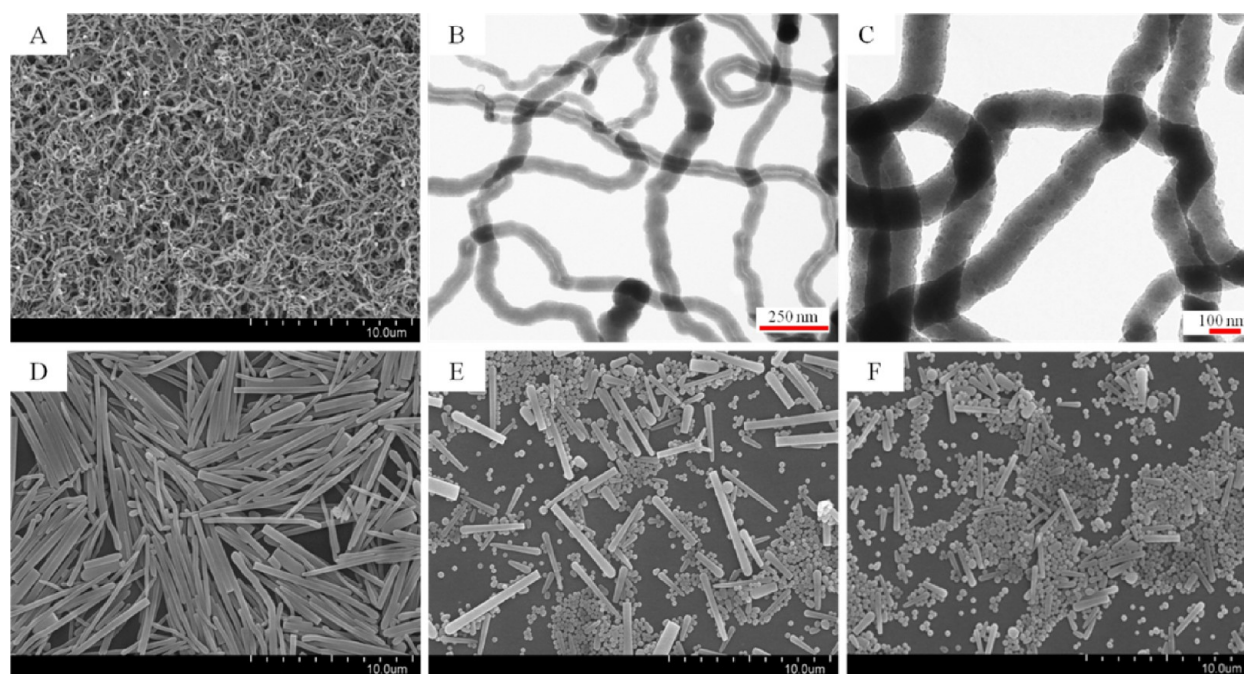
3.1.1. Effect of the Molar Ratio of NH_4OH to TEOS. Analogous to the classic sol−gel process, NH_4OH was used as a basic catalyst for hydrolysis of TEOS. In addition, NH_4OH has also been reported as a morphological catalyst reagent.[31] The amount of NH_4OH in the reaction medium has a pronounced influence on the integrity and surface morphology of the synthesized silica nanomaterials. A wide range of molar ratios of NH_4OH to TEOS (0.53, 1.06, 2.12, 3.18, 4.24, and 5.30) were investigated (Figure 3) in the 1-propanol solvent system. At a low molar ratio of NH_4OH to TEOS (0.53; Figure 3A), hollow crushed-microballoon-like particles with thin shells were obtained. As the molar ratio of NH_4OH to TEOS (1.06) increased, the particles became more spherical with a thicker silica shell. Meanwhile, some of the particles started to grow tails to form tadpole-like structures (Figure 3B). When the molar ratio of NH_4OH to TEOS reached 2.12, a tadpole-like structure formed (Figure 3C). With a further increase in the molar ratio of NH_4OH to TEOS (3.18, 4.24 and 5.30), the head of the particle became more solid while the tail kept the hollow structure and grew longer (Figure 3D,F).
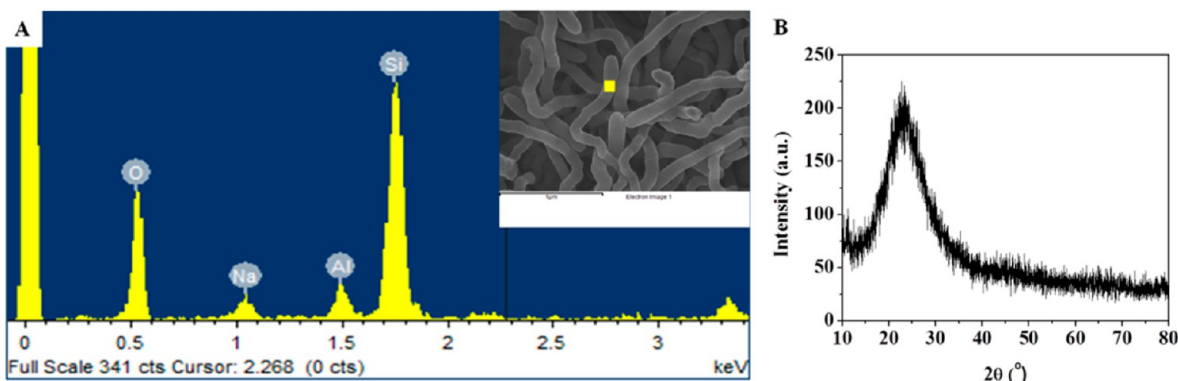
**Figure 2.** EDS spectrum (A) and XRD pattern (B) of the synthesized HSiNWs.
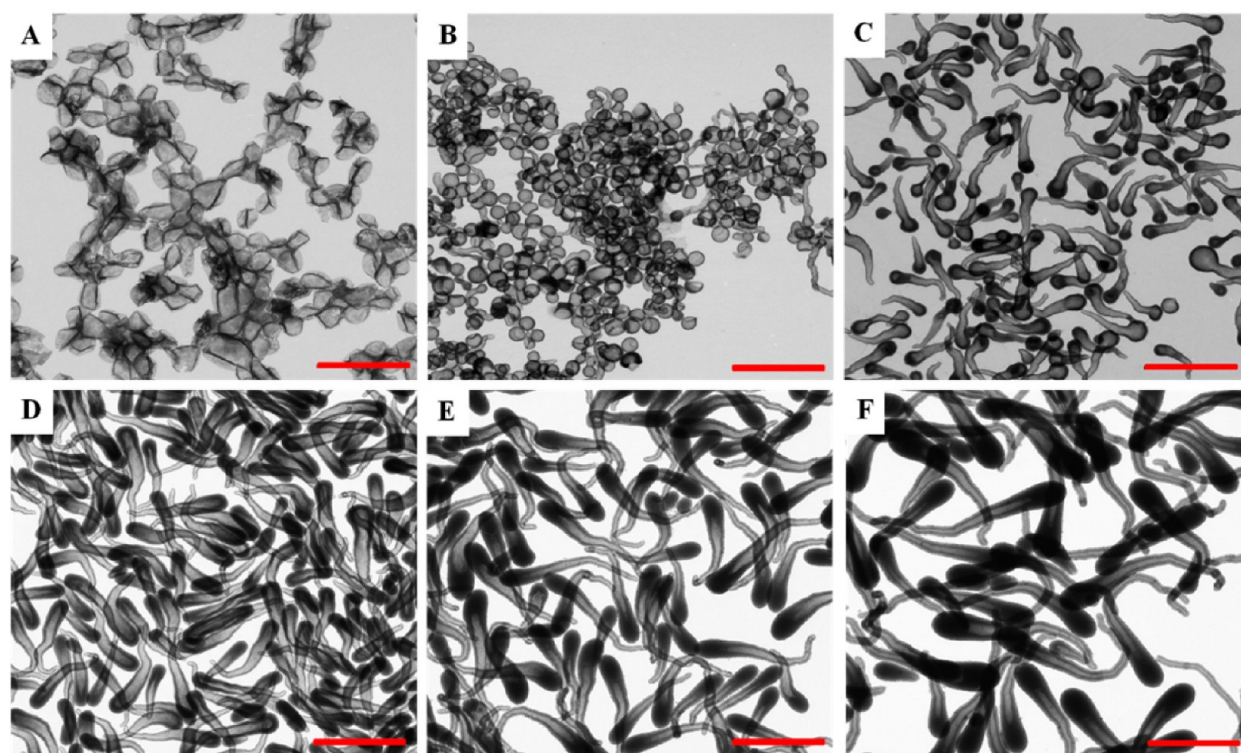
Figure 3. TEM images of the HSNs prepared using 1-propanol under various molar ratios of NH_4OH to TEOS. From A to F, the molar ratio of NH_4OH to TEOS was 0.53, 1.06, 2.12, 3.18, 4.24, and 5.30, respectively (scale bar: 1 μm).


Figure 4. SEM (A and D−F) and TEM (B and C) images of the synthesized silica nanomaterials with a change in the molar ratio of NH_4OH to TEOS from 0.53 (A, B), 1.60 (C), 2.67 (D), 4.80 (E), to 5.87 (F), respectively. 1-Pentanol was used as the solvent.

When 1-pentanol was used as the solvent, ultralong and amorphous HSiNWs were obtained (Figure 4A−C) at relatively low molar ratios (0.53 and 1.60). Differences were revealed under high-magnification TEM images in these two molar ratios of NH_4OH to TEOS (Figure 4B,C). In a molar ratio of 0.53, silica nanowires with hollow nanostructures were obtained (Figure 4B), while only solid nanowires were

synthesized in the molar ratio of 1.60 (Figure 4C). As the molar ratio of NH_4OH to TEOS increased to 2.67, 4.80, and 5.87, solid silica nanorods and nanoparticles were synthesized (Figure 4D−F). The above results might be explained by different TEOS hydrolysis and condensation rates under various NH_4OH to TEOS molar ratios. The condensation of TEOS was fast at low molar ratios of NH_4OH to TEOS, in
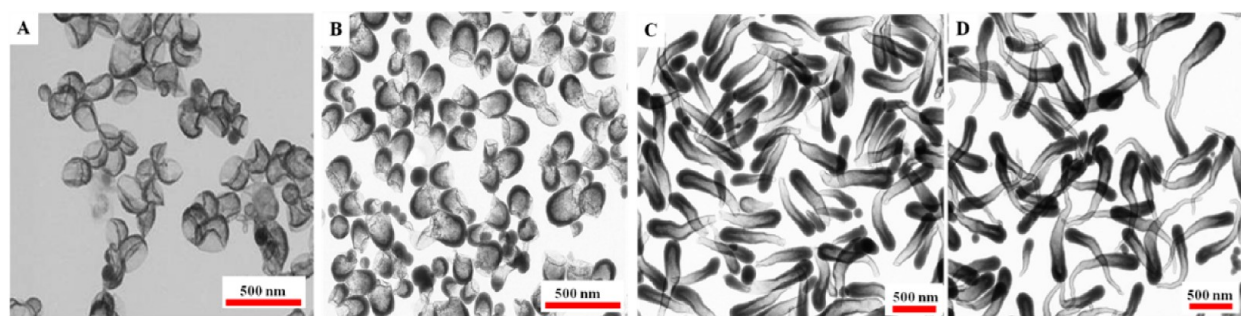
Figure 5. TEM images of the silica tadpole-like nanomaterials in the formation process, preceding the reaction for (A) 5 min, (B) 10 min, (C) 20 min, and (D) 1 h, respectively.
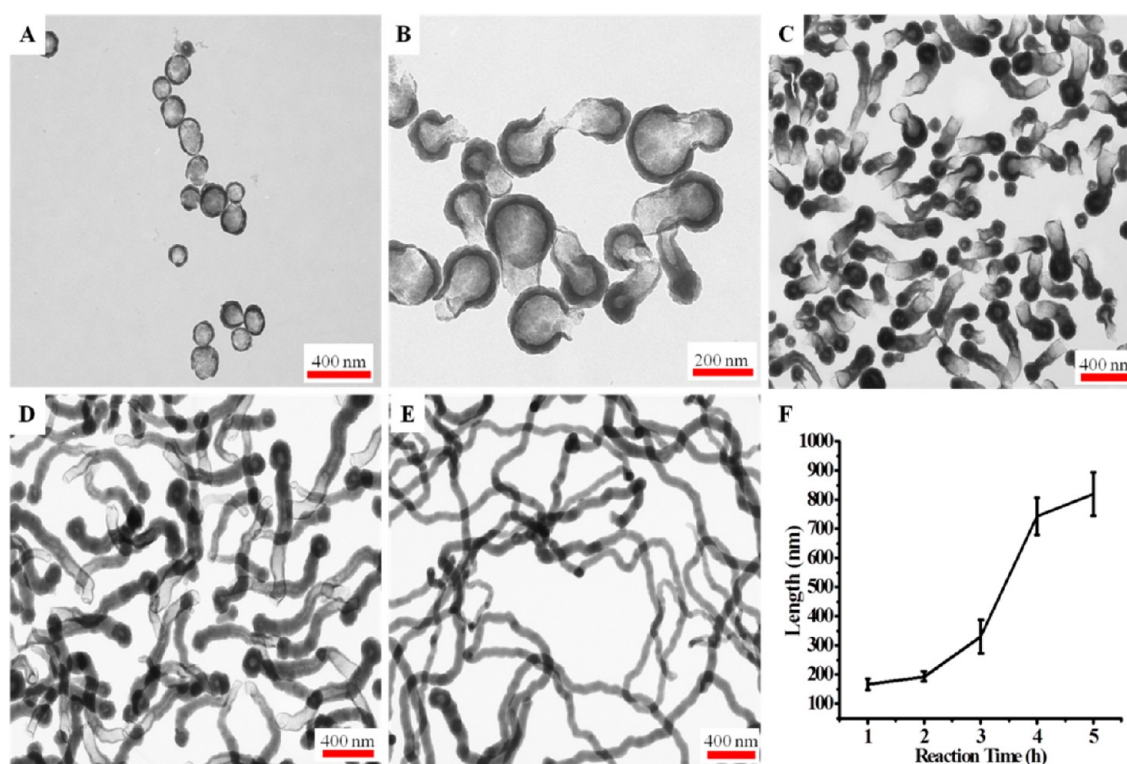
Figure 6. Growth of HSiNWs observed at different reaction times: (A) 1 h; (B) 2 h; (C) 3 h; (D) 5 h; (E) 16 h. (F) Length changes of products versus the reaction time.
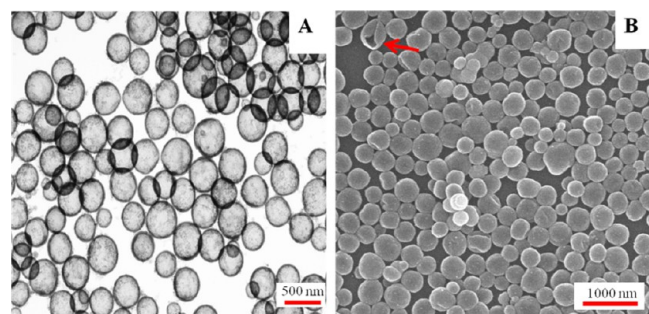

Figure 7. (A) TEM and (B) SEM images of synthesized HSSNs by using EtOH as the solvent.

which the byproducts (EtOH and H_2O molecules) were unable to diffuse into the relatively nonpolar solvent pentanol in a timely manner and were trapped inside the newly formed nanowires. With several washings, the spaces occupied by these encapsulated small byproducts became the hollow parts of the nanowires. The rough surfaces of the HSiNWs also indicated that they were not formed by slow thermodynamically controlled processes. In contrast, the condensation rate probably decreased at a high molar ratio of a NH_4OH aqueous solution to TEOS because of the large excess of NH_4OH and the H_2O introduced at the same time. Therefore, no byproduct or PVP–H_2O mixture was trapped inside the nanomaterials (Figure 4C–F). The observation of solid nanowires, nanorods, and nanoparticles at high molar ratio of NH_4OH to TEOS was consistent with Kuijk et al.'s report.[32] The formation of such long HSiNWs was quite challenging, and the one-pot process reported herein is not only novel but also facile and reliable.

3.2. Formation Process of HNSNs. To study the formation process of the silica nanomaterials in different solvents and propose a possible growth mechanism, the intermediates were collected at different reaction intervals and then characterized using TEM. The intermediates in the synthesis of tadpole-like silica nanmaterials were collected at 5 min, 10 min, 20 min, and 1 h, while 1, 2, 3, 5, and 16 h were
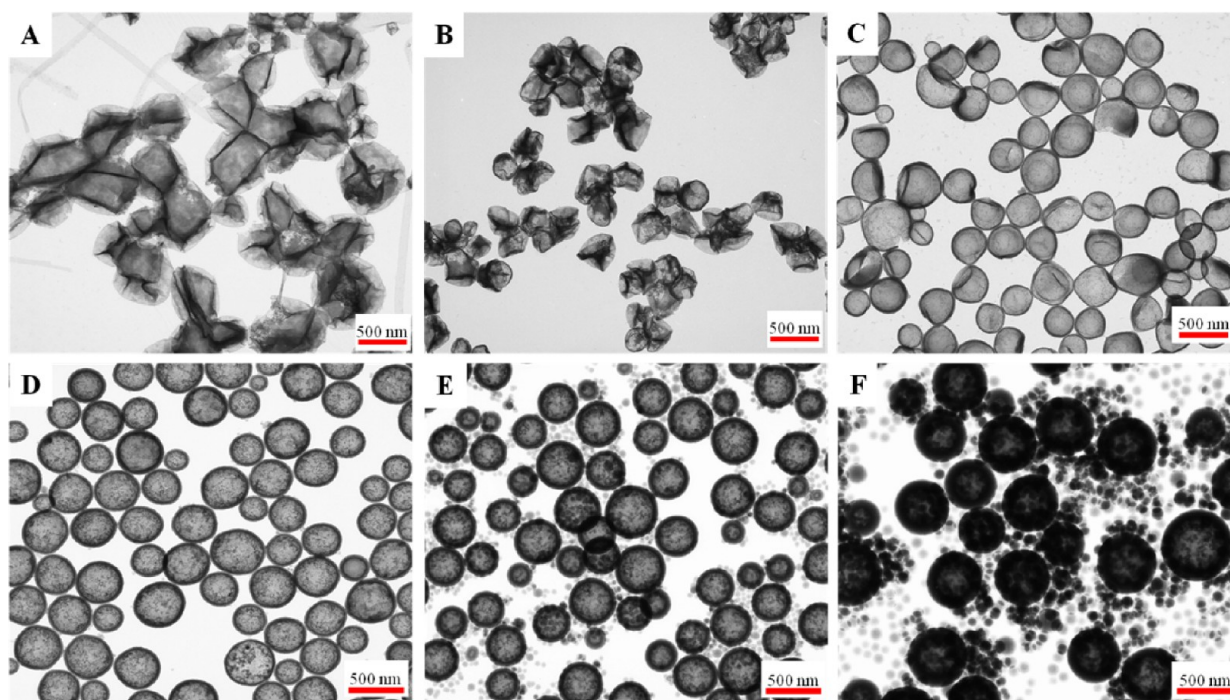
Figure 8. TEM images of the HSSNs prepared under various molar ratios of NH$_4$OH to TEOS by applying EtOH as the solvent. From A to F, the molar ratio of NH$_4$OH to TEOS is 1.06, 2.12, 3.18, 4.24, 5.30, and 6.36, respectively. The experiment was performed by changing the amount of NH$_4$OH, while other conditions were fixed.
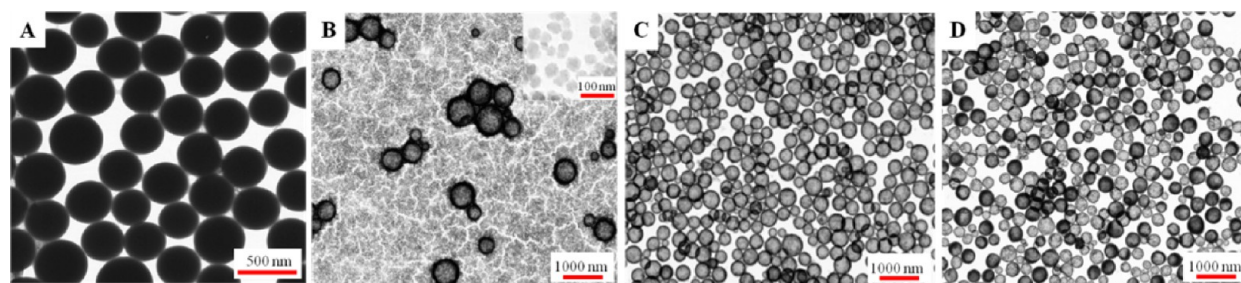
Figure 9. TEM images of silica nanoparticles obtained at different concentrations of PVP: (A) 0 wt %; (B) 31.3 wt %; (C) 62.5 wt %; (D) 125 wt %. Inset image in B: solid silica nanoparticles.

Scheme 1. Formation of Hollow Nanomaterials in Different Solvents: EtOH (1), 1-Propanol (2), and 1-Pentanol (3)
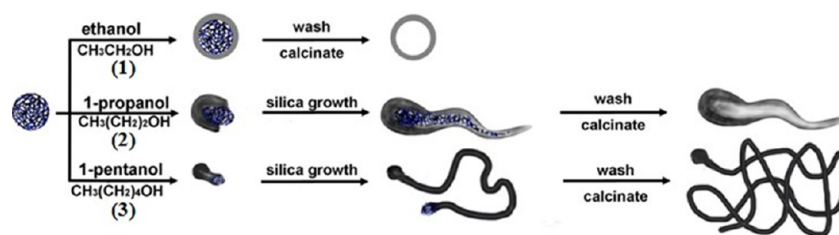
used to collect the intermediates of silica nanowires. The reaction rate was faster in the 1-propanol system than in the 1-pentanol because the synthesis of hollow tadpole-like silica nanomaterials can be finished within 1 h. This probably is due to the steric effects in solvent alcohol. As the molecular weight of the alcohols increases, the steric hindrance becomes important. From these TEM images, the evolution process of the products is clearly revealed.

3.2.1. Hollow Tadpole-like Silica Nanomaterials. At the initial stage (5 min after the addition of TEOS), the products showed hollow hemispheres with one side open (Figure 5A).

After 10 min of reaction, the silica shell grew thicker at one side, forming a head of the tadpole (Figure 5B). With an increase of the reaction time to 20 min, the length of the nanomaterials increased dramatically (Figure 5C) and a hole formed at the tail. The length of the tadpole kept growing within 1 h (Figure 5D) until the hole at the end of the tail was closed. With a further increase in the reaction time to 16 h, the size of the tadpole only showed slight changes.

3.2.2. HSiNWs. At the early stage of hollow nanowire growth (1 h), the produced hollow nanomaterials were more likely to have spherical shapes, as shown in Figure 6A. It is worth noting
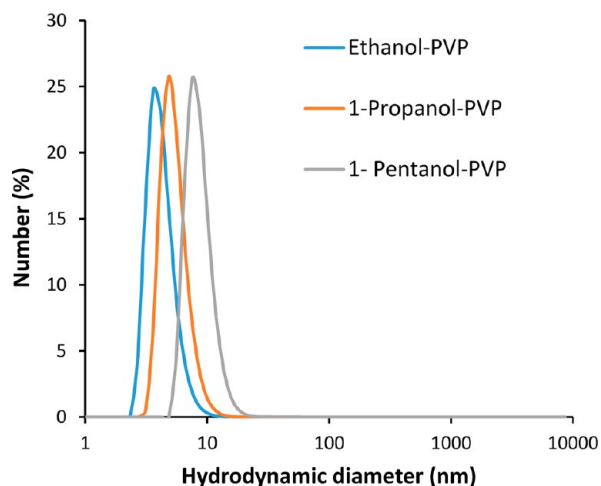
21926

dx.doi.org/10.1021/am507642t | *ACS Appl. Mater. Interfaces* 2014, 6, 21921−21930

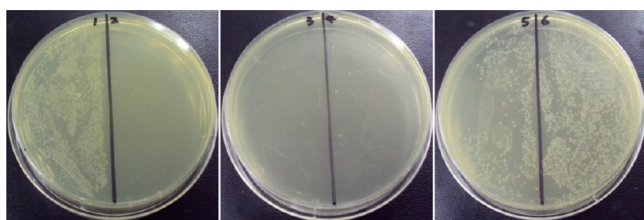**Figure 10.** Hydrodynamic diameter distribution of the PVP solutions.

Figure 11. Antibacterial function of the polymyxin B-doped HSNs toward Gram-negative *E. coli* bacteria. Photographs were taken after incubation for 24 h at 37 °C. The samples (each sample is half of the agar dish) from left to right are (1) pure H_2O, (2−5) polymyxin B-doped HSSNs with concentrations of 0.500, 0.250, 0.125, and 0.050 mg/mL, respectively, and (6) 2.000 mg/mL pure HSSNs.

that the thickness of the silica shell in this stage was not uniform. After 2 h of reaction, a silica tail appeared at the thinner shell area and began to grow along the direction (Figure 6B,C). Long HSiNWs were formed by further reaction until TEOS was completely consumed (Figure 6D,E). The steep increase in the length of the HSiNWs was observed during the first 4 h (Figure 6F). It was difficult to measure the length of HSiNWs after an overnight reaction (16 h) because they were densely tangled. In both 1-propanol and 1-pentanol systems, spherical-like HSNs were formed at the initial stage,

which proved the existence of PVP−H_2O droplets and hydrolysis and condensation on the surface of the droplets.

3.3. Synthesis of HSSNs. The HSSNs could be synthesized by changing the applied solvent to EtOH. As shown in Figure 1, monodispersed HSSNs with a relatively uniform size and a smooth surface were obtained. The average diameter of the particles in Figure 1 was 365 ± 49 nm. The hollow structure of these spherical particles can be revealed by the contrast between the dark outlier and the pale inner in the spheres (Figure 7A). The hollow structure was also observed in broken particles in the SEM image (red arrows in Figure 7B).

3.3.1. Effect of the Molar Ratio of NH_4OH to TEOS. The molar ratio of NH_4OH to TEOS (the amount of TEOS was fixed) was varied from 1.06, 2.12, 3.18, 4.24, 5.30, to 6.36 to study the effect of the molar ratio on the formation of the HSSNs (Figure 8). Without NH_4OH in the reaction system, no nanoparticles were obtained because of slow hydrolysis of TEOS. At low molar ratios of NH_4OH to TEOS (1.06 and 2.12), the products were deformed and aggregated, as shown in Figure 8A,B. The deformed silica structures seemed to be the broken thin-shell HSSNs because they were too fragile to survive during the sequential workup. When the molar ratio was increased to 3.18, a large number of HSSNs were observed (Figure 8C). However, some of them had open ends rather than intact HSSNs. With a further increase in the ratio of NH_4OH to TEOS to 4.24 and 5.30, perfectly intact HSSNs were synthesized (Figure 8D,E). If the molar ratio further increased to 6.36, the majority of the products became solid silica nanoparticles, as shown in Figure 8F, and the silica shell of HSSNs became much thicker. With changing molar ratio of NH_4OH to TEOS, the silica shell thickness increased from 23.02 ± 3.1 nm (Figure 8D), to 32.8 ± 2.2 nm (Figure 8E), to 50.6 ± 2.9 nm (Figure 8F), respectively.

3.4. Role of PVP on the Formation of the Hollow Structure. The effect of the PVP concentration on the formation of hollow nanomaterials was investigated. The HSSNs were taken as an example. In the absence of PVP, solid silica nanoparticles without a hollow interior were obtained as shown in Figure 9A. In the presence of different concentrations of PVP varying from 31.3, to 62.5, to 125 wt %, the HSSNs were successfully synthesized. When the concentration of PVP was 31.3 wt % (Figure 9B), which was lower than the minimum PVP−H_2O binding concentration (57 wt %),[33] there were a limited number of H_2O molecules bound to
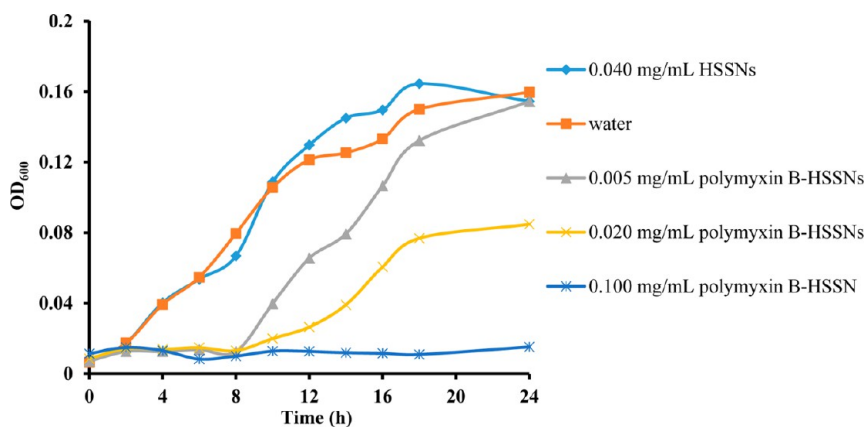

Figure 12. Bacteria growth curves in LB media with pure HSSNs, H_2O, and different concentrations of polymyxin B-doped HSSNs. Wavelength: 600 nm.

PVP. Therefore, the majority of the synthesized nanomaterials were solid silica nanoparticles (inset TEM image in Figure 9B) with a few HSSNs. As the concentration of PVP increased to 62.5 wt %, well-dispersed HSSNs were obtained, as shown in Figure 9C. All hollow nanoparticles appeared as a spherical morphology with uniform size. When the concentration of PVP was further increased to 125 wt % (Figure 9D), no significant morphological change was observed except for a slight decrease in size from 365 ± 49 to 359 ± 55 nm.

3.5. Possible Mechanism. A possible mechanism of the formation of hollow nanomaterials with tunable morphologies was proposed based on the above results (Scheme 1). The formation of PVP−H_2O droplets and the intrinsic properties of applied solvents play critical roles in the synthesis process. PVP is an amphiphilic, nonionic polymer that is soluble in H_2O and many nonaqueous solvents because of the presence of a highly polar amide group within the pyrrolidone ring. Therefore, PVP was commonly viewed as a surfactant and a stabilizer in material synthesis. One important property of PVP is that, at a high concentration of PVP (≥57 wt %) in aqueous solution, H_2O molecules preferred binding with PVP instead of acting as the solvent, which was referred to as bound H_2O.[33] When TEOS was added, its hydrolysis and condensation took place at the interface of the hydrophobic phase and the PVP−H_2O droplets. The hydrolyzed $Si(OH)_x(OCH_2CH_3)_{4-x}$ molecules were polar and tended to accumulate at the oil−H_2O interface of the emulsion. As the hydrolysis and condensation continuously proceeded, the resulting silica assembled on the surface of PVP−H_2O droplets, eventually resulting in a hollow interior after removal of the PVP−H_2O droplets.

The morphology of synthesized nanomaterials changed dramatically with different applied solvents. EtOH is the most commonly used solvent to obtain spherical silica nanoparticles based on TEOS hydrolysis and condensation as follows:[34]

$$Si(OCH_2CH_3)_4 + 4H_2O \leftrightarrow Si(OH)_4 + 4EtOH \qquad (1)$$

$$nSi(OH)_4 \leftrightarrow nSiO_2 + 2nH_2O \qquad (2)$$
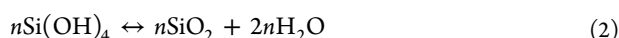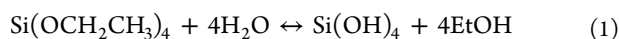
The produced EtOH and H_2O are homogeneously miscible with the solvent EtOH. Thus, the surface tension of PVP−H_2O droplets barely changed. Therefore, perfectly spherical-shaped hollow nanomaterials were obtained in the EtOH−solvent system [Scheme 1(1)]. On the contrary, if the produced EtOH and H_2O are not homogeneously miscible with the solvent, the surface tension of PVP−H_2O droplets would change in the formation of the silica shell; thus, the shape of the PVP−H_2O droplets would change, resulting in different morphologies of the silica shell [Scheme 1(2),(3)].

When 1-propanol was used as the solvent, although it is also miscible with H_2O, the combined solution was far from homogeneous.[35] In this case, some produced H_2O molecules would prefer binding with PVP rather than dispersing into the surrounding solvent. Thus, the surface tension of PVP−H_2O droplets would be changed. As the anisotropic supply continued to hydrolyze and condense, the PVP−H_2O droplets were deformed where the silica grew along, resulting in a tadpole-like shape [Scheme 1(2)].

Unlike EtOH and 1-propanol, which are miscible with H_2O, 1-pentanol is immiscible with H_2O, and its solubility in H_2O is only 2.19 wt %.[36] Therefore, the produced EtOH and H_2O molecules were unable to timely diffuse into the relatively nonpolar solvent pentanol and were trapped inside the newly formed nanowires. The spaces occupied by these encapsulated

small byproducts became the hollow parts of the nanowire after workup. Meanwhile, the PVP−H_2O droplets remained in the end of the nanowire, and the silica continued to grow along the direction, resulting in an ultralong wire-shaped nanostructure [Scheme 1(3)].

To investigate the difference of the PVP−solvent solutions, we measured the hydrodynamic size distribution of the PVP solution in EtOH, 1-propanol, and 1-pentanol using dynamic light scattering. As shown in Figure 10, the hydrodynamic diameters of the PVP solutions increased from EtOH to 1-propanol and 1-pentanol. Even the dynamic light scattering results cannot demonstrate the shape of the formed droplets; the increase in the hydrodynamic diameters indicated the possible shape change when the solvent was varied. From this point of view, the type of solvent will impact the morphology of the resulting silica nanomaterials.

3.6. Potential Applications of the HSNs. Hollow nanomaterials are of great interest for applications in drug delivery and catalysis. To investigate potential applications of the developed hollow nanomaterials, the HSSNs were selected as an example to study its drug-carrying ability. In this work, we studied whether drugs could maintain their activity after being encapsulated in the HSNs.

Polymyxin B, a well-known drug for its biocidal activity on a number of bacteria, was chosen as a model drug. The antimicrobial efficacy of the polymyxin B-doped HSNs was examined against Gram-negative *E. coli* bacteria, which has been used as a model bacterial system for various antimicrobial tests. Without the addition of polymyxin B-doped HSNs, a full bacterial layer on the surface was observed (Figures 1, 6, and 11). However, in the dish with the highest concentration of polymyxin B-doped HSNs (Figures 2 and 11), the dish surface was completely free from bacteria. As the concentration of the polymyxin B-doped HSSNs decreased, bacterial colonies gradually increased (Figures 3−5 and 11).

We further quantitatively evaluated the antibacterial activity of the polymyxin B-doped HSSNs by studying the growth kinetics of bacteria in a LB liquid medium. The bacterial proliferation was measured using OD_{600} based on the turbidity of the cell suspension within 24 h. The growth curve showed a typical concentration-dependent antibacterial effect of the polymyxin B-doped HSSNs (Figure 12). The bacteria growth curves in the presence of polymyxin B-doped HSSNs were significantly different from the ones in the two control media (H_2O and pure HSSNs) in the first 8 h, suggesting strong inhibition of proliferation of *E. coli*. Complete inhibition of *E. coli* growth during the whole 24 h was observed when 0.100 mg/mL polymyxin B-doped HSSNs were used. These data strongly suggest a long-term antibacterial activity of polymyxin B after being doped in the HSSNs.

4. CONCLUSION

In summary, HSNs with different morphologies have been successfully synthesized by simply changing the solvent. By using three different solvents, hollow spherical nanoparticles, tadpole-like nanomaterials, and nanowires were obtained, which further generate a broad family of interesting structures. The morphology of synthesized nanomaterials can also be tuned by the molar ratio of NH_4OH to TEOS and the reaction time. A mechanism based on the intrinsic properties of the solvents, diffusion rates of the side products, and the condensation reaction rate of TEOS was proposed. Overall, the newly developed synthetic process is an efficient one-step

procedure using inexpensive and commercially available reagents, showing high reproducibility and great potential for a large-scale synthesis. Their application as a drug carrier was demonstrated using the hollow spherical silica nanoparticles.

■ AUTHOR INFORMATION

Corresponding Author
*E-mail: jzhao@chem.und.edu. Tel: 701-777-3610.
Notes
The authors declare no competing financial interest.

■ ACKNOWLEDGMENTS

■ REFERENCES

(1) Jung, C. Y.; Kim, J. S.; Chang, T. S.; Kim, S. T.; Lim, H. J.; Koo, S. M. One-Step Synthesis of Structurally Controlled Silicate Particles from Sodium Silicates using a Simple Precipitation Process. *Langmuir* **2010**, *26*, 5456−5461.

(2) Nandiyanto, A. B. D.; Akane, Y.; Ogi, T.; Okuyama, K. Mesopore-Free Hollow Silica Particles with Controllable Diameter and Shell Thickness via Additive-Free Synthesis. *Langmuir* **2012**, *28*, 8616−8624.

(3) Wu, H.; Tang, B.; Wu, P. Novel Hollow Mesoporous Silica Spheres/Polymer Hybrid Membrane for Ultrafiltration. *J. Phys. Chem. C* **2011**, *116*, 2246−2252.

(4) Deng, T.-S.; Marlow, F. Synthesis of Monodisperse Polystyrene@ Vinyl-SiO₂ Core−Shell Particles and Hollow SiO₂ Spheres. *Chem. Mater.* **2011**, *24*, 536−542.

(5) Jin, D.; Lee, J. H.; Seo, M. L.; Jaworski, J.; Jung, J. H. Controlled Drug Delivery from Mesoporous Silica using a pH-Response Release System. *New J. Chem.* **2012**, *36*, 1616−1620.

(6) Young, K. L.; Scott, A. W.; Hao, L.; Mirkin, S. E.; Liu, G.; Mirkin, C. A. Hollow Spherical Nucleic Acids for Intracellular Gene Regulation Based upon Biocompatible Silica Shells. *Nano Lett.* **2012**, *12*, 3867−3871.

(7) Liberman, A.; Martinez, H. P.; Ta, C. N.; Barback, C. V.; Mattrey, R. F.; Kono, Y.; Blair, S. L.; Trogler, W. C.; Kummel, A. C.; Wu, Z. Hollow Silica and Silica-Boron Nano/Microparticles for Contrast-Enhanced Ultrasound to Detect Small Tumors. *Biomaterials* **2012**, *33*, 5124−5129.

(8) Zhai, X.; Yu, M.; Cheng, Z.; Hou, Z.; Ma, P. a.; Yang, D.; Kang, X.; Dai, Y.; Wang, D.; Lin, J. Rattle-Type Hollow CaWO₄: Tb³⁺@SiO₂ Nanocapsules as Carriers for Drug Delivery. *Dalton Trans.* **2011**, *40*, 12818−12825.

(9) Chen, J.; Ding, H.; Wang, J.; Shao, L. Preparation and Characterization of Porous Hollow Silica Nanoparticles for Drug Delivery Application. *Biomaterials* **2004**, *25*, 723−727.

(10) Li, Z.; Xu, S.; Wen, L.; Liu, F.; Liu, A.; Wang, Q.; Sun, H.; Yu, W.; Chen, J. Controlled Release of Avermectin from Porous Hollow Silica Nanoparticles: Influence of Shell Thickness on Loading Efficiency, UV-Shielding Property and Release. *J. Controlled Release* **2006**, *111*, 81−88.

(11) Zhou, J.; Wu, W.; Caruntu, D.; Yu, M. H.; Martin, A.; Chen, J. F.; O'Connor, C. J.; Zhou, W. L. Synthesis of Porous Magnetic Hollow Silica Nanospheres for Nanomedicine Application. *J. Phys. Chem. C* **2007**, *111*, 17473−17477.

(12) Chu, N.; Wang, J.; Zhang, Y.; Yang, J.; Lu, J.; Yin, D. Nestlike Hollow Hierarchical MCM-22 Microspheres: Synthesis and Exceptional Catalytic Properties. *Chem. Mater.* **2010**, *22*, 2757−2763.

(13) Wang, Y.; Tang, C.; Deng, Q.; Liang, C.; Ng, D. H. L.; Kwong, F.-l.; Wang, H.; Cai, W.; Zhang, L.; Wang, G. A Versatile Method for Controlled Synthesis of Porous Hollow Spheres. *Langmuir* **2010**, *26*, 14830−14834.

(14) Qi, G.; Wang, Y.; Estevez, L.; Switzer, A. K.; Duan, X.; Yang, X.; Giannelis, E. P. Facile and Scalable Synthesis of Monodispersed Spherical Capsules with a Mesoporous Shell. *Chem. Mater.* **2010**, *22*, 2693−2695.

(15) Kato, N.; Ishii, T.; Koumoto, S. Synthesis of Monodisperse Mesoporous Silica Hollow Microcapsules and Their Release of Loaded Materials. *Langmuir* **2010**, *26*, 14334−14344.

(16) Blas, H.; Save, M.; Pasetto, P.; Boissière, C.; Sanchez, C.; Charleux, B. Elaboration of Monodisperse Spherical Hollow Particles with Ordered Mesoporous Silica Shells via Dual Latex/Surfactant Templating: Radial Orientation of Mesopore Channels. *Langmuir* **2008**, *24*, 13132−13137.

(17) Tan, B.; Lehmler, H. J.; Vyas, S. M.; Knutson, B. L.; Rankin, S. E. Fluorinated-Surfactant-Templated Synthesis of Hollow Silica Particles with a Single Layer of Mesopores in Their Shells. *Adv. Mater.* **2005**, *17*, 2368−2371.

(18) Yuan, J.; Bai, X.; Zhao, M.; Zheng, L. C₁₂mimBr Ionic Liquid/ SDS Vesicle Formation and Use as Template for the Synthesis of Hollow Silica Spheres. *Langmuir* **2010**, *26*, 11726−11731.

(19) Lin, Y.-S.; Wu, S.-H.; Tseng, C.-T.; Hung, Y.; Chang, C.; Mou, C.-Y. Synthesis of Hollow Silica Nanospheres with a Microemulsion as the Template. *Chem. Commun.* **2009**, *24*, 3542−3544.

(20) Wang, D. P.; Zeng, H. C. Creation of Interior Space, Architecture of Shell Structure, and Encapsulation of Functional Materials for Mesoporous SiO₂ Spheres. *Chem. Mater.* **2011**, *23*, 4886−4899.

(21) Shi, J.; Yao, Q.; Li, X.; Zhou, G.; Fu, S. Controlled Morphogenesis of Amorphous Silica and Its Relevance to Biosilicification. *Am. Mineral.* **2012**, *97*, 1381−1393.

(22) Patwardhan, S. V. Biomimetic and Bioinspired Silica: Recent Developments and Applications. *Chem. Commun.* **2011**, *47*, 7567−7582.

(23) Chen, X.; Berger, A.; Ge, M.; Hopfe, S.; Dai, N.; Gösele, U.; Schlecht, S.; Steinhart, M. Silica Nanotubes by Templated Thermolysis of Silicon Tetraacetate. *Chem. Mater.* **2011**, *23*, 3129−3131.

(24) Wu, X.-J.; Jiang, Y.; Xu, D.; Unique Transformation, A. Route for Synthesis of Rodlike Hollow Mesoporous Silica Particles. *J. Phys. Chem. C* **2011**, *115*, 11342−11347.

(25) Wang, S.; Zhang, M.; Wang, D.; Zhang, W.; Liu, S. Synthesis of Hollow Mesoporous Silica Microspheres through Surface Sol−Gel Process on Polystyrene-*co*-poly(4-vinylpyridine) Core−Shell Microspheres. *Microporous Mesoporous Mater.* **2011**, *139*, 1−7.

(26) Wang, Y. W.; Liang, C. H.; Meng, G. W.; Peng, X. S.; Zhang, L. D. Synthesis and Photoluminescence Properties of Amorphous SiOₓ Nanowires. *J. Mater. Chem.* **2002**, *12*, 651−653.

(27) Zhu, Y. Q.; Hu, W. B.; Hsu, W. K.; Terrones, M.; Grobert, N.; Karali, T.; Terrones, H.; Hare, J. P.; Townsend, P. D.; Kroto, H. W.; Walton, D. R. M. A Simple Route to Silicon-Based Nanostructures. *Adv. Mater.* **1999**, *11*, 844−847.

(28) Jiang, Z.; Xie, T.; Yuan, X. Y.; Geng, B. Y.; Wu, G. S.; Wang, G. Z.; Meng, G. W.; Zhang, L. D. Catalytic Synthesis and Photoluminescence of Silicon Oxide Nanowires and Nanotubes. *Appl. Phys. A: Mater. Sci. Process.* **2005**, *81*, 477−479.

(29) Lee, K.-H.; Lofton, C.; Kim, K.; Seo, W.-S.; Lee, Y.; Lee, M.-H.; Sigmund, W. Photoluminescence from Amorphous Silica Nanowires Synthesized using TiN/Ni/SiO₂/Si and TiN/Ni/Si Substrates. *Solid State Commun.* **2004**, *131*, 687−692.

(30) Kim, J. H.; Yoon, C. S. Amorphous Silicon Dioxide Nanowire Array Synthesized via Carbonization of Polyimide Thin Film. *J. Phys. Chem. C* **2008**, *112*, 4463−4468.

(31) Byers, C. H.; Harris, M. T.; Williams, D. F. Controlled Microcrystalline Growth Studies by Dynamic Laser-Light-Scattering Methods. *Ind. Eng. Chem. Res.* **1987**, *26*, 1916−1923.

(32) Kuijk, A.; van Blaaderen, A.; Imhof, A. Synthesis of Monodisperse, Rodlike Silica Colloids with Tunable Aspect Ratio. *J. Am. Chem. Soc.* **2011**, *133*, 2346−2349.

(33) de Dood, M. J. A.; Kalkman, J.; Strohhöfer, C.; Michielsen, J.; van der Elsken, J. Hidden Transition in the "Unfreezable Water" Region of the PVP−Water System. *J. Phys. Chem. B* **2003**, *107*, 5906−5913.

(34) Chen, S.-L.; Dong, P.; Yang, G.-H.; Yang, J.-J. Characteristic Aspects of Formation of New Particles during the Growth of Monosize Silica Seeds. *J. Colloid Interface Sci.* **1996**, *180*, 237−241.

(35) Yang, H. G.; Zeng, H. C. Creation of Intestine-like Interior Space for Metal-Oxide Nanostructures with a Quasi-Reverse Emulsion. *Angew. Chem., Int. Ed* **2004**, *43*, 5206−5209.

(36) Thimons, K. L.; Brazdil, L. C.; Harrison, D.; Fisch, M. R. Effects of Pentanol Isomers on the Growth of SDS Micelles in 0.5 M NaCl. *J. Phys. Chem. B* **1997**, *101*, 11087−11091.